Multiscale Computation of Polymer Models

Dov Bai

Achi Brandt
Department of Computer Science
And Applied Mathematics
The Weizmann Inst. of Science, Rehovot 76100, Israel

Abstract. We present a multiscale algorithm and preliminary numerical results for Monte-Carlo (MC) simulations of simple polymers. Fine level MC simulations on a small number of points are used for constructing a coarse level Hamiltonian in, generally, an iterative process. The main criterion for selecting terms for coarse Hamiltonian is the preservation of local quantities such as probability distributions and correlations of internal variables on the scale of the coarse level. We demonstrate that coarse level simulations with the coarse Hamiltonian reproduce correctly the distribution of a longer range quantity, the end-to-end distance. Two types of chain molecules are discussed: (1) A chain with bonding forces only and (2) a chain with Lennard-Jones forces. In the first case terms expressing distributions and correlations of internal coordinates are sufficient. In the second case explicit coarse Lennard-Jones terms are added to the Hamiltonian.

1. Introduction

Simulation of long polymers (and generally all macromolecules) is one of the most computationally intensive tasks. This is due mostly to the large variation in time scales (10^{-15} seconds to several hours) and length scales (1Å-1000Å) involved in each problem. While much of the interesting behavior occurs at longer time (or length) scales, the shorter scales, where the basic equations are given, constrain the size of steps in simulations. However, by applying multiscale methods these constraints can be removed as different physical scales are resolved on corresponding appropriate computational levels.

In this work we present some results and guidelines for developing multiscale Monte-Carlo (MC) algorithms for modeling polymers. See §1.1 for a brief mathematical formulation of the problem. A summary of intermediate results is presented in §14.6 of [13]. For alternative coarsening schemes using coarse grained models see [14].

The basic process is the construction of a coarse level Hamiltonian. The coarse Hamiltonian can then be used very efficiently to calculate observables on the scale of the coarse level. This process may continue recursively to increasingly coarser scales. The strategy is to calculate local terms of the coarse Hamiltonian by using simulations at the fine level which involve only a local set (typically several dozens) of neighboring points (or atoms, or monomers, or any other basic units in terms of which the fine level is formulated). Short range interactions between points of the local set and those outside are ignored: this does not significantly affect the accuracy of the coarse Hamiltonian terms located sufficiently inside (several atomic distances from the margin of) the local set.

This approach is similar to the one used in Algebraic Multigrid (AMG) methods [8, 4, 1, 5] and in Renormalization Multigrid (RMG) [6, 7].

Long range electrostatic interactions can be decomposed into the sum of short-range interactions and *smooth* interactions. The latter can be transferred directly to the coarse level, using the method of [9] (see Sec. 4).

The coarse Hamiltonian is constructed iteratively. In each iteration a large number of MC steps over the local set are made with the current Hamiltonian, calculating various observables and comparing them to corresponding values obtained by simulations at the fine level. The difference is then used to get a better coarse Hamiltonian.

New terms are added gradually to the coarse Hamiltonian. The important criterion is the ability of the existing terms to provide good approximations to various observables defined on the coarse points of the local set. The added terms correspond in general to strong local correlations which are not well reproduced by the current coarse Hamiltonian.

1.1 Problem Formulation: simple polymers

Our purpose here is to demonstrate the general approach outlined above on simplified models of polymers.

A polymer consists of repeat units (typically $10^3 - 10^5$) of chemical groups of atoms, called *monomers*. Simple non-branching polymers have a structure of chain molecules with their monomers located at the nodes of the chain. This is the kind of polymers discussed in this work. An example is polymethylene whose monomers are atomic groups of CH_2. For comprehensive discussion of chain molecules see [3].

In simple polymer models (e.g. "united atom") monomers are considered as a single unit and details of their internal structure and interactions are ignored. Mathematically, the monomers are represented as points.

The configurations of chain molecules are conveniently described by using 3 types of internal variables. In Fig. 1 a chain molecule with 9 points is plotted. These points are numbered $1, \ldots, 9$. The first type of internal variables is the *bond-length* which is the distance between two adjacent chain points. In Fig. 1 $r_{2,3}$, the distance between points 2, 3 is an example of a bond-length. The second type of variables is the *bond-angle* formed by a group of 3 adjacent chain points. In Fig. 1 $\theta_{3,4,5}$ is a bond-angle formed by points $3, 4, 5$. The third type of internal variables is the *dihedral angle* which is formed by 4 adjacent points. It is the angle between two intersecting planes defined by 3 of the 4 points. For example, in Fig. 1, $\phi_{6,7,8,9}$ the dihedral angle formed by points $6, 7, 8, 9$ is the angle between two planes: the first contains the points $6, 7, 8$ and the second $7, 8, 9$.

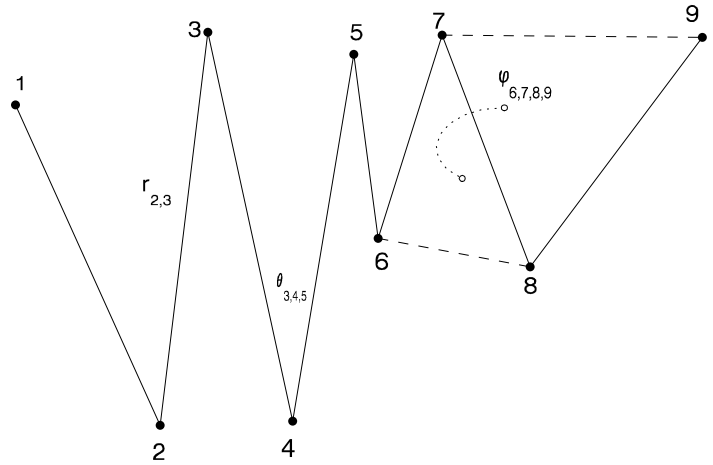

Fig. 1: Chain molecule

There are two types of interactions between monomers: bonded and non-bonded. Bonded interactions are the stronger ones. They are intramolecular, keeping the monomers of the chain together and provide its basic structural properties. They are normally expressed in terms of the 3 types of internal variables. The strongest interaction is between any pair of adjacent points and expressed in terms of bond-lengths. A weaker bonded interaction is expressed in terms of bond angles and the weakest in terms of dihedral angles. The latter plays an important role in longer-range chain conformations (configurations).

The second type of molecular interactions are the non-bonded ones. These are usually weaker and are both intra- and inter-molecular. Example are Lennard-Jones (Van der Waals) and electrostatic interactions. Simple models for polymethylene take into account only Lennard-Jones (LJ) forces, as we do in this work.

2. Bonded-Only Chain

In this section we describe detailed results of deriving a coarse level Hamiltonian for a polymethylene-like bonded chain without Lennard-Jones forces (which will be added in §3). The chain consists of n identical monomers located at positions $r_1, \ldots, r_n$. The fine level interaction terms are taken from [2]:

1. $C-C$ bond-length energy, $K_s(r-r_0)^2$, where r is a bond length, $r_o = 1.52\mathring{A}$, $K_s = 500 Kcal/mol/\mathring{A}^2$.
2. $C-C-C$ Bond-angle energy, $1/2 K_\theta(\cos\theta - \cos\theta_0)^2$, where θ is a bond angle, $\theta_0 = 110°$, $K_\theta = 120$ $Kcal/mol$.
3. $C-C-C-C$ torsion (depicted in Fig. 2)

$$\frac{1}{2}[K_\phi^1(1-\cos\phi) + K_\phi^2(1-\cos 2\phi) + K_\phi^3(1-\cos 3\phi)]$$

where ϕ is a dihedral angle, $K_\phi^1 = 1.6 Kcal/mol$, $K_\phi^2 = -0.867 Kcal/mol$, $K_\phi^3 = 3.24 Kcal/mol$.

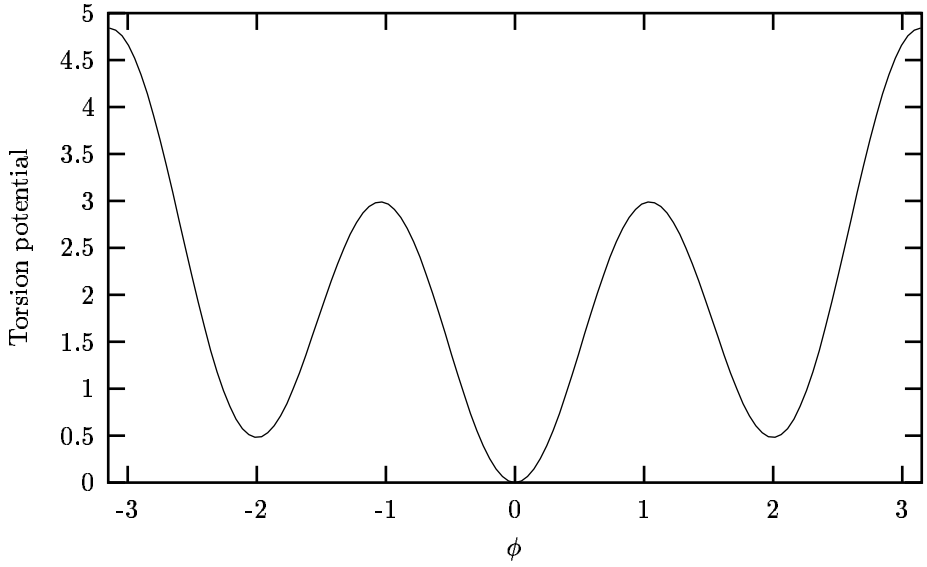

Fig. 2: Dihedral torsion potential

The overall fine-level Hamiltonian H^B of the chemical bonds is thus given by

$$\begin{aligned} H^B(r_1,\ldots,r_n) = &\sum_{i=1}^{n-1} \frac{1}{2} K_s(r_{i,i+1} - r_0)^2 \\ &+ \sum_{i=1}^{n-2} \frac{1}{2} K_\theta(\cos\theta_{i,i+1,i+2} - \cos\theta_0)^2 \\ &+ \sum_{i=1}^{n-3} \frac{1}{2} \left[K_\phi^1(1-\cos\phi_{i,i+1,i+2,i+3}) + K_\phi^2(1-\cos 2\phi_{i,i+1,i+2,i+3}) + K_\phi^3(1-\cos 3\phi_{i,i+1,i+2,i+3})\right]. \end{aligned} \tag{2.1}$$

The probability distribution of the configurations is given by $\exp(-H^B(r_1,\ldots,r_n)/k_BT)$, where T is the absolute temperature and k_B is Boltzmann's constant. Our simulations were all made at room temperature.

2.1 Coarsening

The coarse level is composed of N coarse points $(r_1^c, \ldots, r_N^c)$, each of which is the center of mass of a group of points on the fine level. In this work a single coarse point is the average location of 4 fine points (coarsening ratio of $1:4$), so $N = n/4$. For instance, if the fine chain contains 12 points numbered $1, \ldots, 12$, (smaller dots in Fig. 3) the coarse level would contain 3 points (larger dots in Fig. 3) at positions $r_i^c = (r_{4i-3} + r_{4i-2} + r_{4i-1} + r_{4i})/4$, $(i = 1, 2, 3)$.

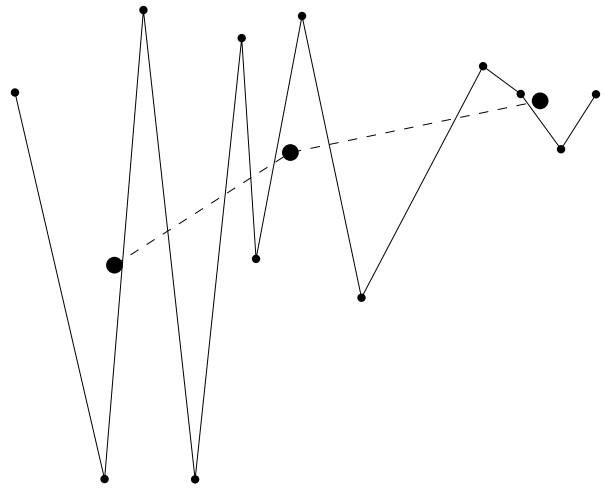

Fig. 3: Coarsening

A coarse level configuration is described by the same kind of internal variables as the fine level: (1) coarse bond-length $R_{i,i+1}$ is the distance $|r_i^c - r_{i+1}^c|$ between coarse atoms i and $i+1$, (2) coarse bond-angle $\Theta_{i,i+1,i+2}$ is formed by coarse atoms i, $i+1$ and $i+2$ and (3) coarse dihedral angle $\Phi_{i,i+1,i+2,i+3}$ formed by coarse point i, $i+1$, $i+2$ and $i+3$.

In this work, the local set is composed of 24 fine points, corresponding to 6 coarse points. Using the bonded potentials (2.1), MC iterations are performed on the 24 local set points. For efficiency, these simulations are made by changing a single fine internal coordinate at a time. For each fine level configuration, the corresponding coarse configuration is calculated: Values of coarse internal coordinates, end-to-end (ETE) distance $|r_1^c - r_N^c|$, as well as other quantities are measured, and their statistics (distribution functions, averages, correlations, etc.) are accumulated. Typically, 300,000 MC iterations are performed, each typically includes a single pass over all internal coordinates.

In Fig. 4, distribution functions of coarse bond-length, bond-angle and dihedral angle are plotted. Because of the symmetry and absence of non-bonded forces in the fine-level Hamiltonian studied here, the distribution of all coordinates of the same type (e.g. bond-lengths) are virtually the same. The solid line in Fig. 5 describes the coarse ETE probability distribution.

These coarse distributions are much less sharp than those of the fine internal variables. In addition $-\log p(U_i)$, where U_i is a coarse internal coordinate and $p(U_i)$ is its probability distribution, does not exhibit significant local minima like the triple minima of the fine torsion potential. As a result, MC iterations are much easier on the coarse level, and allow much longer steps.

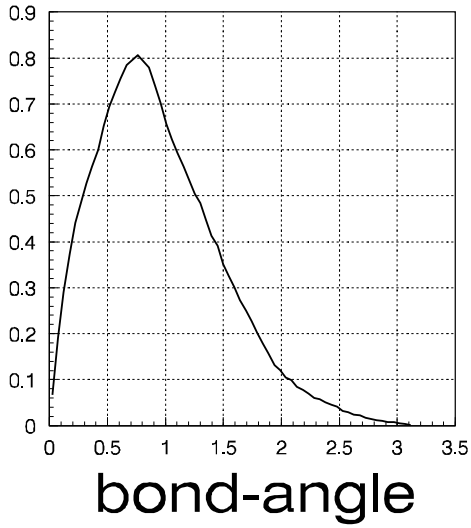

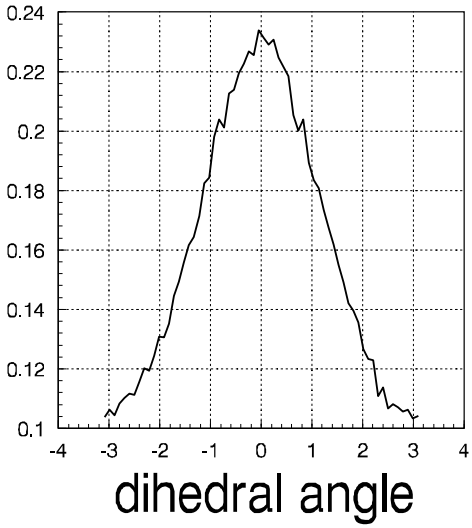

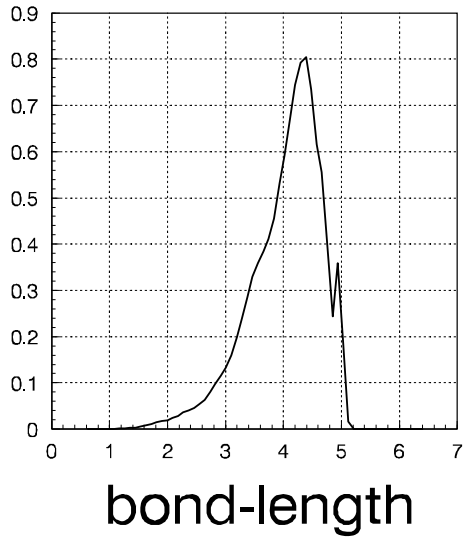

Fig. 4: Coarse chain probability distributions in the absence of Lennard-Jones interactions.

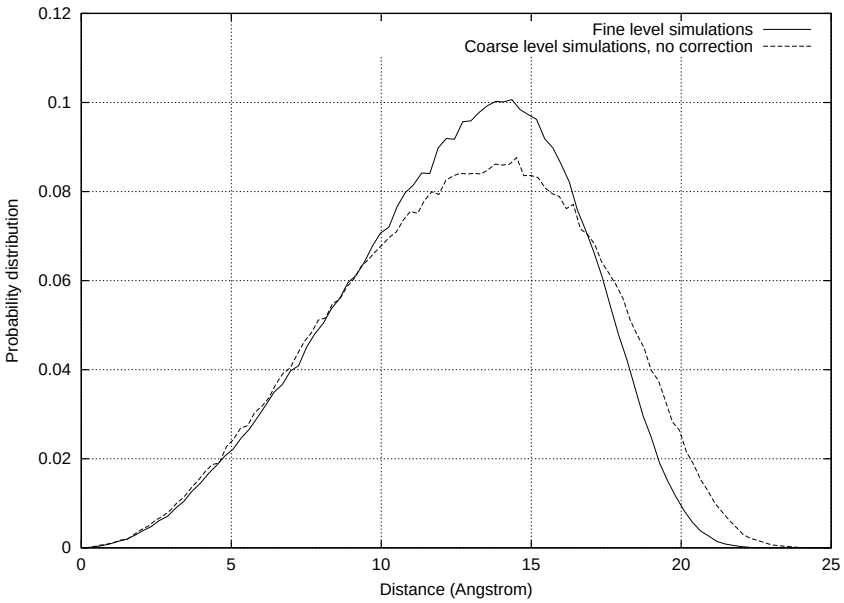

Fig. 5: End-to-end probability distributions in the absence of LJ

2.2 Coarse Hamiltonian

In general, the coarse Hamiltonian H^c can be expressed as a sum of operators H_k, each multiplied by a corresponding real parameters A_k,

$$H^c = \sum_k A_k H_k. \tag{2.2}$$

A simple Hamiltonian may be constructed by expressing the terms H_k as binary functions (with values 0 or 1). For example, consider an internal coordinate U_i. Assume that all values of U_i are in an interval I_i. The interval I_i is divided into smaller subintervals I_i^j. With each such subinterval a Hamiltonian term $A_k H_k = \beta_i^j B(U_i, j)$ can be associated, where $A_k = \beta_i^j$ is a real number and

$$H_k = B(U_i, j) = \begin{cases} 1, & \text{if } U_i \epsilon I_i^j \\ 0, & \text{otherwise.} \end{cases} \tag{2.3}$$

Note that $B(U_i, j)$ is an operator and its average value $< B(U_i, j) >$ is an observable whose value is the probability of U_i to be in the subinterval I_i^j.

The description of probability distributions as discontinuous piecewise-constant functions (sums of binary terms as above) is of course not the most efficient. Better accuracy with fewer terms can be obtained by, e.g., continuous *piecewise-linear* functions. In this case each H_k is a "tent" function

$$H_k = H_{i,j} = B(U_i, j) = \begin{cases} 0 & \text{if } U_i \le X_{j-1}^i \\ \frac{U_i - X_{j-1}^i}{X_j^i - X_{j-1}^i} & \text{if } X_{j-1}^i \le U_i \le X_j^i \\ \frac{X_{j+1}^i - U_i}{X_{j+1}^i - X_j^i} & \text{if } X_j^i \le U_i \le X_{j+1}^i \\ 0 & \text{if } X_{j+1}^i \le U_i \end{cases} \qquad (j = 1, \ldots, n_i - 1), \tag{2.4}$$

where $X_0^i < X_1^i < \ldots X_{n_i}^i$ is a grid placed over the interval $I_i = [X_0^i, X_{n_i}^i]$. One can calculate with these linear elements (or with similar, even higher-order elements) as easily as with the binary ones.

For two similar molecular coordinates in a similar molecular neighborhood it is useful to attach just one parameter. For example, in our current simple chain without Lennard-Jones interactions, the same distribution can be assumed for all coarse lengths $R_{i,i+1}$, $(i = 0, \ldots, N-1)$. For efficiency in collecting statistics they should therefore all be described by one *collective Hamiltonian term.* Thus, instead of using

individual Hamiltonian terms $H_{ij} = B(R_{i,i+1}, j)$ of the type described above (either (2.3) or (2.4)), a collective term such as

$$H_j^{(R)} = \sum_{i=1}^{N-1} B(R_{i,i+1}, j), \qquad (j = 1, 2, \ldots m_R),$$

is employed, having one collective parameter $A_j^{(R)}$ as a coefficient. Similar collective coarse Hamiltonian terms

$$H_j^{(\Theta)} = \sum_{i=1}^{N-2} B(\Theta_{i,i+1,i+2}, j), \qquad (j = 1, 2, \ldots, m_\Theta)$$

and

$$H_j^{(\Phi)} = \sum_{i=1}^{N-3} B(\Phi_{i,i+1,i+2,i+3}, j), \qquad (j = 1, 2, \ldots, m_\Phi)$$

are defined for angles and dihedrals, respectively, m_R, m_Θ and m_Φ being of course the number of collective parameters (e.g., the number of subintervals) associated with every length, angle and dihedral, respectively. Thus the overall coarse Hamiltonian can for now be written as

$$\begin{aligned} H^c &= \sum_{k=1}^{K} A_k H_k \qquad (2.5) \\ &= \sum_{j=1}^{m_R} A_j^{(R)} H_j^{(R)} + \sum_{j=1}^{m_\Theta} A_j^{(\Theta)} H_j^{(\Theta)} + \sum_{j=1}^{m_\Phi} A_j^{(\Phi)} H_j^{(\Phi)} \end{aligned}$$

where $K = m_R + m_\Theta + m_\Phi$.

We denote by $< H_k >_f$ and $< H_k >_c$ the values of the observable $< H_k >$, the average of H_k, obtained in fine and coarse simulations, respectively. As a first approximation to the coarse Hamiltonian we choose A_k so that, under the assumption of mutual independence of internal coordinates, each of their probability distributions would match the one found at fine-level simulations. In the case of (2.3), for example, this means

$$A_k = -k_B T \log < H_k >_f / |I_k|, \qquad (2.6)$$

where $|I_k|$ is the length of I_i^j (which can be taken to equal 1 if it does not depend on i). Coarse level MC iterations performed with this Hamiltonian would produce probability distributions of internal variables which may be rather close to the correct (fine) distributions (i.e. $< H_k >_c \approx < H_k >_f$). However, this may not be close enough. Also, other observables may not be reproduced sufficiently well.

Fig. 5 describes the ETE probability distribution of the local set obtained (a) in fine level simulations (solid line) and (b) with this first coarse Hamiltonian (dashed line). If the difference between these two curves, or any other error, is considered too large, the Hamiltonian (2.5) should be corrected, either by adjusting the parameters A_k or by adding new terms.

In the coarse Hamiltonian (2.5) all correlations between internal coordinates are vanishing. The new terms are chosen such that various correlations between terms are correctly obtained on the coarse level.

For brevity we denote in the following discussion the bond-angle $\Theta_{i,i+1,i+2}$ and bond-length $R_{j,j+1}$ by Θ_i and R_j respectively.

The strongest (relative) correlation measured by fine-level simulations is between a coarse angle and the two lengths forming it (e.g., Θ_1 and R_1 or R_2). The relative correlation between the pair Θ_i, R_j is defined by

$$C_{al}(i,j) = (< \Theta_i R_j > - < \Theta_i >< R_j >)/(\sqrt{(< \Theta_i^2 > - < \Theta_i >^2)(< R_j^2 > - < R_j >^2)}$$

In numerical experiments we find that $C_{al}(i,j)$ is nearly vanishing unless $j = i$ or $j = i+1$. For $j = i, i+1$ the relative correlations are a constant (independent of j) whose value is -0.45. We denote this constant by C_{al}. To match this correlation we add to the coarse Hamiltonian a corresponding correlation term $c_{al} H^{al}$, where c_{al} is a parameter generally different from C_{al} and

$$H^{al} = \sum_{i=0}^{N-2} \sum_{j=i}^{i+1} (\Theta_i - < \Theta_i >_f)(R_j - < R_j >_f), \qquad (2.7)$$

where $< \Theta_i >_f$ and $< R_j >_f$ are the fine averages of Θ_i and R_j.

Just adding $c_{al}H^{al}$ to the simple Hamiltonian (2.5) would generally change distributions of coarse internal coordinates. To get the correct distributions it would be necessary also to modify the parameters $A_j^{(R)}$, $A_j^{(\Theta)}$ and $A_j^{(\Phi)}$ of (2.5). A general scheme for obtaining corrections to Hamiltonian terms can be derived from the following general formula for the perturbation $\delta < O >$ in any observable $< O >$ resulting from a small perturbation δH in the Hamiltonian:

$$\delta < O >= [< O >< \delta H > - < O \cdot \delta H >] / k_B T. \tag{2.8}$$

For a general Hamiltonian (2.2), the corrections δA_l to the parameters A_l should therefore generally be obtained by solving the linear system

$$< H_k >_f - < H_k >_c = \frac{1}{k_B T} \sum_l (< H_k >< H_l > - < H_k H_l >) \delta A_l \tag{2.9}$$

for all k. $\langle H_k \rangle_c$ is of course the average of the operator H_k calculated with the *current* (before correction) coarse-level Hamiltonian, while $\langle H_k \rangle_f$ is the corresponding average computed by fine level simulations. The averages on the right of (2.9) can be calculated on either the fine or the coarse levels. More generally, they can be just approximated, since they only serve as iteration coefficients. In fact, one can ignore most of these terms, only those should be calculated that correspond to neighboring coordinates which might be significantly correlated.

An advisable approach is to calculate $< H_k H_l >$ for those potentially-corrected operators *both on the fine and the coarse level*. Even when the iterations (2.9) have converged, i.e., $< H_k >_f - < H_k >_c$ is sufficiently small for all H_k included in the coarse Hamiltonian (2.2), for some pairs (k,l) one may still find that $< H_k H_l >_f - < H_k H_l >_c$ is still large. This can be corrected by adding the term $A_{kl} H_k H_l$ to the coarse Hamiltonian and returning to the iterations (2.9) to find the value of A_{kl} (and of any other similarly added correlation coefficient) while also simultaneously readjusting the old parameters A_k. This gives a general scheme for both calculating the parameters of H^c and detecting what terms need be added to it.

In the preliminary results presented here, however, we did not actually make full use of this general scheme. Also, except for (2.7) no collective Hamiltonian terms were used: H_k was either of the form (2.3) or (2.7). The coarse Hamiltonian was examined through the following iterative process: Denote by $c_{al}(k)$, $\beta_i^j(k)$ the values of c_{al}, β_i^j (see (2.3)) used at the k-th iteration and by $< B(U_i, j) >_{c,k}$ the coarse level averages of the operators $B(U_i, j)$ obtained at that k-th iteration. At the first iteration $c_{al}(1) = 0$ and $\beta_i^j(1) = -k_B T \log < B(U_i, j) >_f / |I_i^j|$ (see (2.6)). At the $(k+1)$-th iteration we simply took

$$c_{al}(k+1) = c_{al}(k) + 0.1$$

and

$$\beta_i^j(k+1) = \beta_i^j(k) - k_B T \log \left[< B(U_i, j) >_{c,k} / < B(U_i, j) >_f \right]. \tag{2.10}$$

Assuming that for β_i^j all non-diagonal terms in the system (2.9) are vanishing, $|I_i^j|/|I_i| \ll 1$ and

$$|(< B(U_i, j) >_{c,k} / < B(U_i, j) >_f) - 1| \ll 1,$$

and using, following (2.3), the relation $B(U_i, j)^2 = B(U_i, j)$, (2.10) is the same as the correction derived from (2.9).

At each iteration the angle-length correlation, $C_{al}(k)$, was measured. The iterative process stopped at the k_0-th iteration for which $C_{al}(k_0) \approx -0.45$.

Table 1 describes the results of the iterative process. k is the iteration number. In the second column $c_{al}(k)$ is listed. The third column describes the measured values $C_{al}(k)$ of the angle-length correlation obtained in the k-th iteration. The last 4 columns describe the error in probability distribution function for ETE, bond-length (R), bond-angle(Θ) and dihedral angle (Φ) distributions compared to their corresponding fine values. The error in the probability density $E(u)$ of a variable u is defined as $\int |P_f(u) - P_c(u)| du$, where $P_f(u)$, $P_c(u)$ are the probability distributions calculated by fine-level and coarse-level simulations,

respectively. Clearly, as C_{al} reaches the fine level value of -0.45 the error in all 4 quantities is very small. This justifies the assumption that the cause of inadequate ETE coarse distribution with the simple Hamiltonian is due to the lack of correlation terms.

Table 1. Coarse Hamiltonian iterations

k	$c_{al}(k)$	$C_{al}(k)$	$E(ETE)$	$E(R)$	$E(\Theta)$	$E(\Phi)$
1	0.0	0.00	0.129	0.012	0.013	0.011
2	0.1	-0.03	0.123	0.018	0.019	0.015
3	0.2	-0.07	0.111	0.018	0.018	0.014
4	0.3	-0.10	0.103	0.020	0.018	0.012
5	0.4	-0.14	0.089	0.020	0.021	0.014
6	0.5	-0.18	0.079	0.022	0.022	0.014
7	0.6	-0.22	0.068	0.024	0.022	0.013
8	0.7	-0.25	0.060	0.022	0.025	0.014
9	0.8	-0.28	0.053	0.025	0.028	0.016
10	0.9	-0.31	0.048	0.027	0.027	0.015
11	1.0	-0.34	0.046	0.024	0.028	0.017
12	1.1	-0.38	0.033	0.031	0.030	0.015
13	1.2	-0.40	0.063	0.026	0.029	0.016
14	1.3	-0.44	0.031	0.035	0.037	0.014

Note that in general adding new Hamiltonian correlation terms may introduce new correlations which do not exist at the fine level. If that happens, corresponding Hamiltonian terms must be added to eliminate these correlations. While no significant correlations were introduced by adding the term (2.7), such correlations did enter in the Lennard-Jones case (§3).

3 Lennard-Jones forces

In this section we discuss the construction of a coarse level Hamiltonian with Lennard-Jones forces added to the fine level. For a pair of fine-level atoms i, j the Lennard-Jones potential [2] is

$$U(r_{ij}) = \begin{cases} \epsilon\left[(\sigma/r_{ij})^{12} - 2(\sigma/r_{ij})^{6}\right] - U(2\sigma), & \text{if } r_{ij} \le 2\sigma, \\ 0, & \text{if } r_{ij} > 2\sigma, \end{cases} \tag{3.1}$$

where r_{ij} is the distance between atoms i and j, $\sigma = 4.5\mathring{A}$, $\epsilon = 0.09344\, Kcal/mol$. Indices i, j denote location on a chain. In the results presented in this chapter Lennard-Jones forces are taken into account for all pairs with $|i-j| \ge 4$.

In Fig. 6, distributions of coarse level internal coordinates as well as ETE of the 6 points local set are described. These are fine level measurements. Note that because of the presence of LJ forces, different distributions of the same type (e.g. bond-angles) are not all identical. For example, out of the 4 coarse angles two are close to the chain ends (marked "external" in Fig. 6) while the other two are internal.

As in §2, correlations between internal coordinates were measured. Table 2 lists relative correlations for the same local set. The first 6 lines of table 2 shows the strongest correlations. The last 3 lines of the Table lists some weak correlations, for comparison.

Table 2. Coarse relative correlations (with LJ forces)

i	:	1	2	3	4
$\Theta_{i,i+1,i+2} \leftrightarrow R_{i,i+1}$	:	-0.37	-0.45	-0.48	-0.45
$\Theta_{i,i+1,i+2} \leftrightarrow R_{i+1,i+2}$	:	-0.45	-0.48	-0.46	-0.37
$\Theta_{i,i+1,i+2} \leftrightarrow \Theta_{i+1,i+2,i+3}$	:	0.14	0.17	0.14	
$\lvert\Phi_{i,i+1,i+2,i+3}\rvert \leftrightarrow R_{i+1,i+2}$	:	0.27	0.31	0.27	
$\lvert\Phi_{i,i+1,i+2,i+3}\rvert \leftrightarrow \Theta_{i,i+1,i+2}$	:	-0.29	-0.31	-0.24	
$\lvert\Phi_{i,i+1,i+2,i+3}\rvert \leftrightarrow \Theta_{i+1,i+2,i+3}$	:	-0.24	-0.31	-0.29	
$\lvert\Phi_{i,i+1,i+2,i+3}\rvert \leftrightarrow R_{i,i+1}$	:	< 0.05	< 0.05	< 0.05	
$\lvert\Phi_{i,i+1,i+2,i+3}\rvert \leftrightarrow R_{i+2,i+3}$	:	< 0.05	< 0.05	< 0.05	
$R_{i,i+1} \leftrightarrow R_{i+1,i+2}$	:	< 0.05	< 0.05	< 0.05	< 0.05

The first two lines in Table 2 list correlations between bond-angles and the bond-lengths forming them. The third line describes correlations between two adjacent bond-angles. The correlations between non-adjacent bond-angles were found to be very small. The next 5 lines describe correlations between absolute values of dihedral angles and other internal variables. Note that because of the symmetry of dihedral angle distributions, their absolute values are taken in correlation calculations.

3.1 Coarse Lennard-Jones terms

The effect of LJ forces on coarse configurations can not be represented correctly by distribution and correlation functions alone as in §2. Thus, explicit Lennard-Jones forces are added to the coarse Hamiltonian.

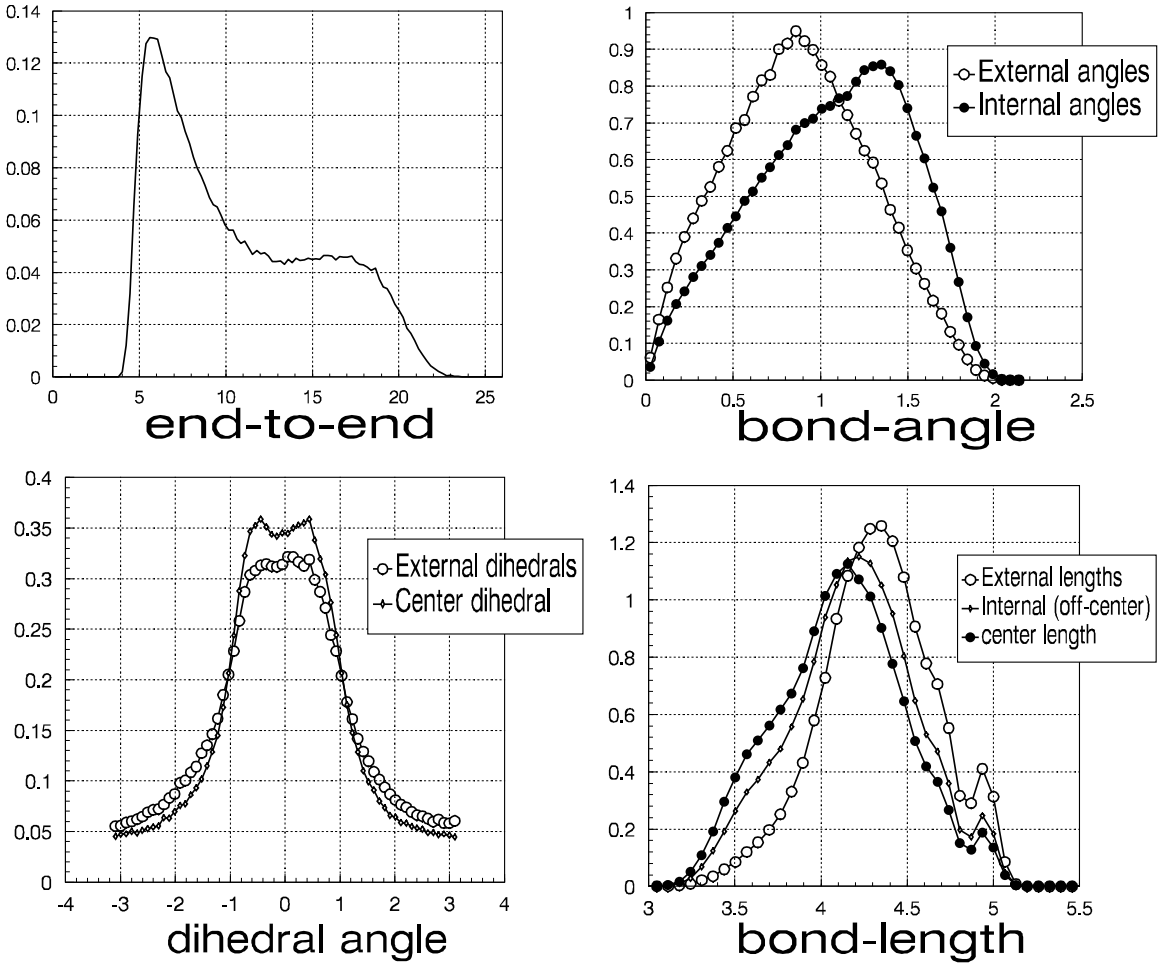

Fig. 6: Distributions of coarse quantities (with LJ)

The general procedure for deriving coarse LJ terms is as follows. The purpose is to derive an energy function which depends only on the distance $R_{ij} = |r_i^c - r_j^c|$ between two coarse points i, j. For each fine configuration and each pair (i,j), the distance R_{ij} is measured together with a corresponding quantity (to be discussed) g that depends on the eight relevant fine points (the four points corresponding to i and the four corresponding to j). Using suitable bins, statistics for $< g >$ as function of R_{ij} is gathered during the fine-level MC runs. In practice, excluding the case $|i-j| = 1$, the dependence of $< g > (R_{ij})$ on the pair (i,j) is rather weak, so the statistics for different pairs can be unified (i.e., collected into the same bins), yielding a general function $< g > (R)$.

Two approaches have been tried: g_1 denotes the measured function g in the first approach, g_2 in the second.

The function g_1 is the sum of the 16 LJ potentials corresponding to the pair of coarse points. That is, denoting the set of fine points corresponding to the i-th coarse point (§2.1) by $s_i = (4i-3, 4i-2, 4i-1, 4i)$,

we measure, for each pair i,j, the quantity

$$g_1 = \sum_{k \epsilon s_i} \sum_{l \epsilon s_j} U(r_{kl}), \tag{3.2}$$

where r_{kl} is the distance between points k, l and $U(r_{kl})$ is the LJ potential (3.1). In this approach $< g_1 >$ (R_{ij}) is the coarse LJ potential function $U^c_{ij}(R_{ij})$.

The solid line in Fig. 7 shows a typical coarse level energy functional derived with this approach.

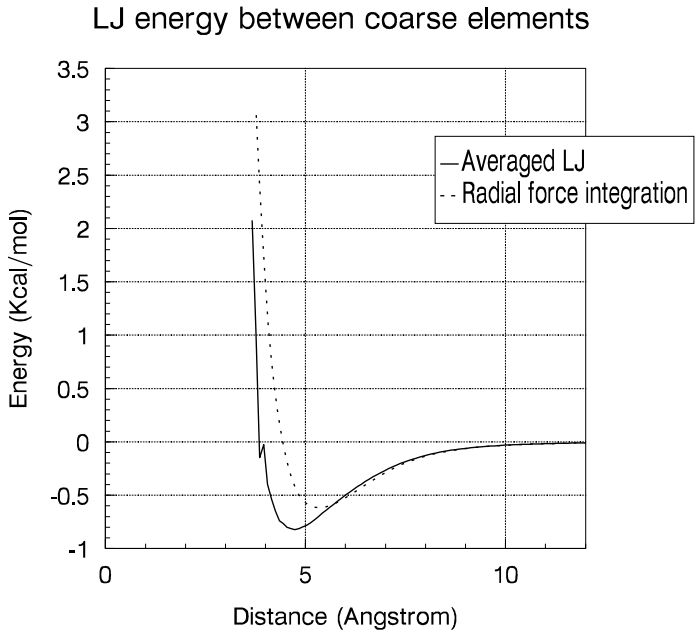

Fig. 7: LJ energy function

Comparing the minimum of the solid line in Fig. 7 and the ETE distribution in Fig. 6 it is obvious that the minimum of the coarse LJ energy term occurs at a shorter distance than the maximum in the ETE distribution.

The second approach tries to correct this situation. In this approach, radial LJ forces rather than LJ energy terms are being measured on the fine level. For two coarse points i, j and their corresponding sets of fine points s_i, s_j, the quantity

$$g_2 = \sum_{k \epsilon s_i} \sum_{l \epsilon s_j} \vec{\nu}_{ij} \cdot \nabla_l U(r_{kl}) \tag{3.3}$$

is measured, where ν_{ij} is the unit vector in the direction $r^c_j - r^c_i$, and ∇_l is the gradient with respect to r_l. The coarse LJ potential function is obtained by numerical integration:

$$U^c_{ij}(R_{ij}) = \int < g_2 > (R_{ij}) dR_{ij}. \tag{3.4}$$

The dotted line of Fig. 7 describes a typical LJ function produced by the second method. Comparing the location of the minimum of the graph with the maximum of the ETE distribution in Fig. 6, it is clear that the two occur at almost the same point. The results of coarse MC steps (to be described later) with this LJ term provide a very good agreement with the fine level simulations near the maximum of the ETE distribution.

3.2 Coarse Hamiltonian

The general form of the coarse Hamiltonian is again as in (2.2), with 3 types of terms. The first type, generally non-collective,

$$\beta_i^j B(U_i, I_i^j) \tag{3.5}$$

where β_i^j are parameters, $B(u_i, I_i^j)$ are the same as in (2.3).

The second type includes correlation terms (§2.2), whose aim is to make coarse level correlations match their corresponding fine level correlations. For example, in the results presented here there are at least 6 types of such terms, corresponding to the six strong correlations between pairs of coordinates as shown in Table 2. A term which expresses correlation between two internal coordinates U_i, U_j is:

$$H^c_{corr(U_i,U_j)} = c_{U_iU_j}(U_i - < U_i >_f)(U_j - < U_j >_f) \tag{3.6}$$

where $c_{U_iU_j}$ is a parameter. The coarse Hamiltonian should include terms like this for all strong correlations. Such correlation terms may often be written collectively (see §2.2) by using a single coefficient $c_{U_iU_j}$ for many pairs U_i, U_j. For example, in the chain described in §3, a single coefficient is used for the correlation terms between the pairs $\Theta_{1,2,3}$, $R_{1,2}$ and $\Theta_{4,5,6}$, $R_{5,6}$ (cf. Table 2) where points 1 and 6 are the first and last points of the chain. As discussed in §2.2, new coarse Hamiltonian terms corresponding to the strong correlations in Table 2 may introduce new strong correlations which did not exist before. This actually happened in our numerical experiments with LJ forces, where new correlations between adjacent lengths appeared. These were eliminated by adding a corresponding correlation term to H^c.

In principle, strong correlations may appear between more specific *subintervals* of neighboring coarse coordinates, i.e., between $B(U_i, j)$ and $B(U_{i'}, j')$, as defined by (2.3), for some particular pairs of subintervals I_i^j and $I_{i'}^{j'}$. This may lead to the introduction to H^c of corresponding subinterval-specific correlations terms. An indication for the need for such terms would automatically show up when statistics is gathered for the system of equations (2.9). However, in our experiments we did not find subinterval-specific correlation terms to be necessary.

LJ interactions are included in the third type. For coarse points i, j, the LJ term is:

$$H^c_{LJ(i,j)} = U^c_{ij}(R_{ij}), \tag{3.7}$$

as derived in §3.1. Note that this term does not include adjustable parameters. In principle, such parameters could be introduced, to fine-tune the accurate reproduction of various distance statistics by the coarse Hamiltonian.

In general the parameters β_i^j and $c_{U_iU_j}$ in (3.5), (3.6) should be determined simultaneously (e.g. iteratively, using (2.9)). However, we have not yet implemented this process in full. Much of the adjustment of parameters has been done manually in the iterative process. In results presented here all strong correlations (Table 2) are being reproduced on coarse level and all distribution functions of internal coordinates are the same as those obtained on fine level.

In Fig. 8 the ETE distribution with LJ forces derived by the first method (Eq. 3.2) are described. The same function $U^c_{ij}(R_{ij})$ (Eq. 3.7) was used for $|i-j| \geq 3$. No LJ terms were used for $|i-j| < 3$.

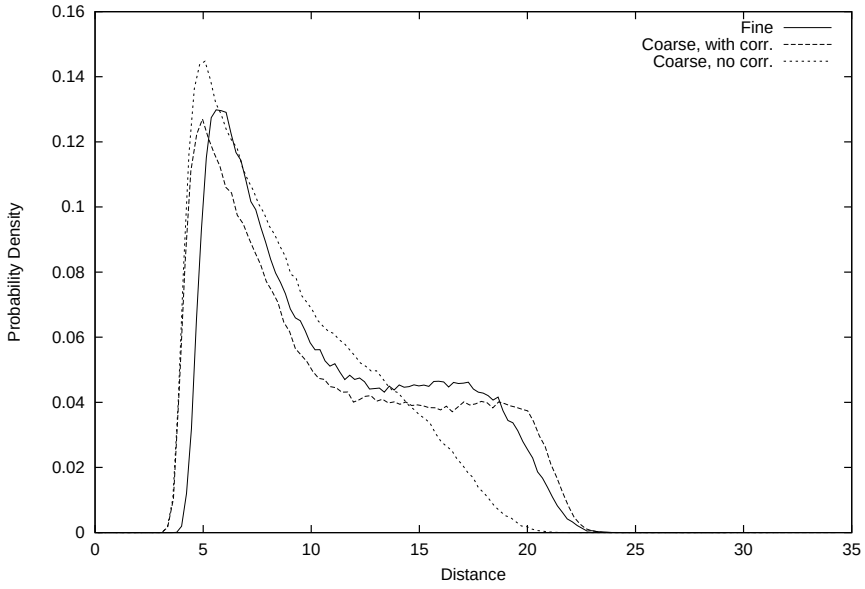

Fig. 8: ETE distributions, Averaged LJ

The solid line describes the fine ETE distribution. The dashed line describes the ETE distribution obtained on the coarse level at convergence (i.e. after all strong correlations and internal coordinate distributions are the same as their corresponding fine values). The dotted line shows the coarse ETE obtained with no coarse iterative process with all correlation coefficients in Eq. (3.6) set to zero and $\beta_i^j = -T \log < B(U_i, I_i^j) >_f$. Clearly, the dotted results are inadequate.

Fig. 9 displays ETE results with coarse LJ terms calculated by the second method (3.4) at convergence. The LJ functions $U_{ij}^c(R_{ij})$ in Eq. (3.7) are different for differing values of $|i-j|$.

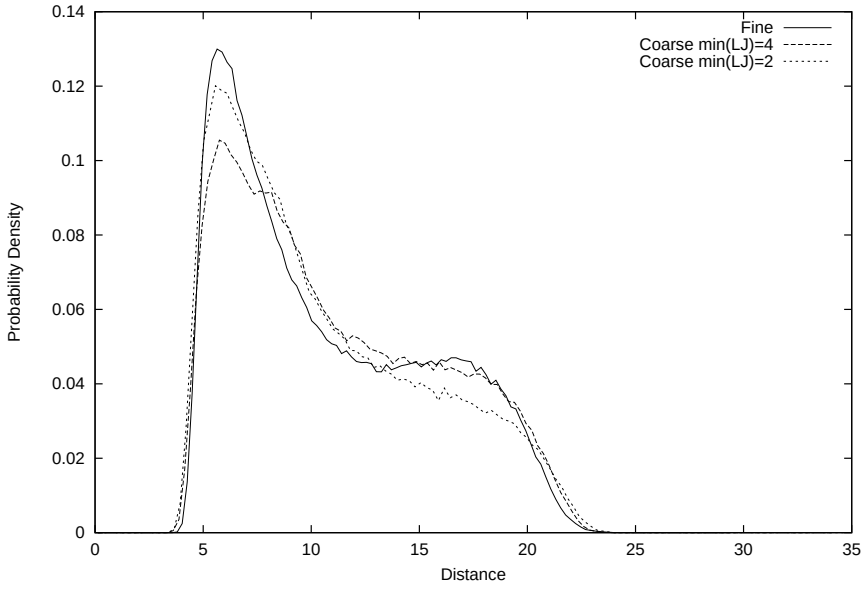

Fig. 9: ETE distributions, integrated radial LJ

The solid line describes the fine ETE. The dashed line shows the ETE distribution obtained with coarse LJ terms only for $|i-j| = 4, 5$. The dotted line describes results with coarse LJ terms for $|i-j| = 2, 3, 4, 5$.

The small inaccuracies in the end-to-end distribution shown here are completely harmless. They may indicate, though, that more severe inaccuracies may show up at meeting regions between two different polymers, or between two remote parts of the same polymer. It is not apriori clear that the current form of the coarse LJ interaction will describe such meeting regions accurately enough. If this happens, however, the coarsening scheme described here will most probably be able to mend the problem by introducing an additional term to the coarse Hamiltonian which depends, e.g., on a local angle between coarse points in the two polymers. Such terms can be found by local MC simulations with two quite short polymers, checking which angle distributions or which correlations in the meeting regions do not fit sufficiently well their fine-level-simulation values.

4. On long-range interactions

A general scheme has been described above for deriving a coarse-level Hamiltonian where the given fine-level Hamiltonian involves only local interactions (chemical bonds and Lennard-Jones). To add the long-range electrostatic interactions to this scheme it is proposed to decompose each two-body electrostatic potential into the sum of two parts: a smooth potential and a local potential. (See details of such decompositions, for charge and for dipolar interactions, in [10].) The charges or dipoles will then be *anterpolated* to the coarse level. (Anterpolation is the adjoint of interpolation; see, e.g., Sec. 3 of [9] or Sec. 3.2 of [10].) In the specific scheme described above, for example, this means to aggregate all the charges and dipoles at each group of four fine-level points to the coarse point at their mass center. This will give good coarse-level approximation to the *smooth* potentials.

Unlike the fast summation schemes based on the same principle, in which charges/dipoles are anterpolated to a *fixed* lattice (as in [9], [10]), here they will be anterpolated to points that *move* during the coarse-level simulations. As a result, the field produced by the coarse-level charges/dipoles will continue to well approximate the fine-level *smooth* potentials even under large global movements of the (coarse) molecule.

It thus remains only to describe at the coarse level the *local* parts of the electrostatic potentials. Being local, these interactions can be added to the local scheme described above, similar to the LJ interactions.

With this approach no explicit electrostatic summations is necessary, especially if (for extra accuracy) the local MC simulations are made in a *distributive* manner (cf. [11]). This means, e.g., to move two particles at a time in such a way that their mass center remains unchanged. such (and *higher-order*) distributive moves are hardly affected by the smooth interactions.

Such distributive moves make of course sense in a multilevel dynamics, where mass centers that remain fixed during the fine level motions are moved at the coarse level. In this framework, the distributive moves can also serve to reduce the cutoff distance for calculating LJ interactions.

5. Hamiltonian corrections through local refinements

For any given coarse level configuration one can produce the fine-level configurations represented by it, with the correct probabilistic weights, by a process we call *stochastic interpolation* or *compatible Monte Carlo (CMC)*. By this we mean a Monte Carlo process at the fine level which is restricted to the subset of the fine-level configurations which are compatible with the given coarse level, i.e., the mass center $(r_{4i-3}+r_{4i-2}+r_{4i-1}+r_{4i})/4$ of each group of four fine points is held fixed at the corresponding point r_i^c of the given coarse configuration.

Such a CMC process equilibrates very fast. (Its decorrelation time is independent of the size of the simulated system.) Otherwise, the choice of coarse-level variables has been wrong, since they do not fully determine, up to local processing, all the fine level equilibrium configurations (Cf. the discussion of CMC in [7] and [12]). Thus, only few CMC passes are needed to perform the interpolation.

The fast CMC equilibration also implies that the interpolation can be done *locally*, over a restricted part of the chain that serves as a *window*: in the window interior, good fine-level equilibrium is reached after few local CMC passes. Holding the window boundaries compatible with the current coarse configuration, further *regular* (not compatible) MC can then be performed in the window interior, to accumulate there new fine-level statistics. Then one can return to the coarse level (replacing its configuration in the window with the average locations of the latest fine-level configuration) and resume the coarse-level simulations.

Such temporary window refinements can be used for further iterative improvement of the coarse Hamiltonian H^c. Indeed, our H^c has been derived in terms of *local sets* (rather short pieces of polymers). It is only with such local sets that efficient simulations can be done, because we can then change one local coordinate at a time while keeping all others fixed (which requires a rotation of a large part of the entire simulated chain), making it possible, for example, to easily sample the different local minima of each potential associated with a fine-level dihedral angle. Although rather accurate terms of the H^c emerge at the interior of the local set, they should be checked and possibly corrected by simulating larger systems (longer chains, and more of them).

Larger systems can only be efficiently simulated at the coarse level, due to its reduced number of variables and, more important, due to the much larger steps allowed by H^c compared with those allowed by the fine-level Hamiltonian H. This is because a well coordinated collective motion can be much larger than the motion allowed for a single particle in a chain, and because in H^c the fine-level local minima have been averaged out (see, e.g., Fig. 4).

So the proposed scheme is to simulate *increasingly larger systems with increasingly coarse Hamiltonians*, and to recursively use windows of larger systems at which finer-level simulations are temporarily resumed, to check and improve the coarse-level Hamiltonian. The larger system prods the local set in the window into new situations, providing more statistics, especially for the various *correlation* terms that couple the local coordinates to each other.

Iterating this way back and forth between the various levels of the system, self-consistency can quickly be reached, establishing accurate Hamiltonians at all levels, while employing only local sets and fast sampling at each level.

Acknowledgements

The authors thank Dr. Ruth Pachter of the US Air Force Research Laboratory (AFRL) for discussions and assistance in carrying out this work. The research has been supported by AFOSR and the Materials and Manufacturing Directorate, AFRL, Wright-Patterson Air Force Base, contract No. F33615-97-D-5405, by Israel Science Foundation grant No. 696/97, and by the Carl F. Gauss Minerva Center for Scientific Computation at the Weizmann Institute of science.

References

[1] J. W. Ruge, K. Stüben, *Algebraic multigrid*, in Multigrid Methods, SIAM Frontiers in Applied Mathematics, 1987.

[2] W. Paul, D.Y. Yoon, G.D. Smith, *An optimized united atom model for simulations of polymethylene melts*, J. Chem. Phys. **103**(4), 1995, pp. 1702-1709.

[3] Paul J. Flory, *Statistical mechanics of chain molecules*, January 1989, ISBN 1569900191.

[4] A. Brandt, S. McCormick, J. Ruge, *Algebraic multigrid (AMG) for automatic multigrid solution with application to geodetic computations*, Institute for Computational Studies, POB 1852, Fort Collins, Colorado, 1982.

[5] A. Brandt, *General highly accurate algebraic ¡coarsening schemes*, Electronic Trans. Num. Anal. **10** (2000) pp. 1-10.

[6] A. Brandt, D. Ron, *Renormalization Multigrid (RMG): Statistically optimal renormalization group flow and coarse-to-fine Monte Carlo acceleration*, Gauss Center Report W1/GC11, June, 1999. J. Stat. Phys., to appear.

[7] A. Brandt, D. Ron, *Renormalization Multigrid (RMG): Coarse-to-fine Monte Carlo acceleration and optimal derivation of macroscopic descriptions.* In this Proceedings.

[8] A. Brandt, S. McCormick, J. Ruge, *Algebraic multi-grid (AMG) for sparse matrix equations*, in Sparsity and its Applications, D.J. Evans, ed., Cambridge University Press, Cambridge, 1984, pp. 257-284.

[9] A. Brandt, *Multilevel computations of integral transforms and particle interactions with oscillatory kernels*, Comput. Phys. Comm. **65** (1991), pp. 24-38.

[10] B. Sandak, A. Brandt, *Multiscale fast summation of long range charge and dipolar interactions*, this Proceedings.

[11] A. Brandt, A.A. Lubrecht, *Multilevel matrix multiplication and fast solution of integral equations*, J. Comput. Phys. **90** (1990), pp. 348-370.

[12] A. Brandt, V. Ilyin, *Multilevel approach in statistical physics of liquids*, this Proceedings.

[13] A. Brandt, *The Gauss Center Research Report in Multiscale Scientific Computation: Six Year Summary*, Gauss Center Report WI/GC-12, May, 1999.

[14] J. Baschnagel, K. Binder, P. Doruker, A.A. Gusev, O. Hahn, K. Kremer, W. L. Mattice, F. Müller-Plathe, M. Murat, W. Paul, S. Santos, U. W. Suter, V. Tries *Bridging the gap between atomistic and coarse-grained models of polymers: Status and Perspectives*, Advances in Polymer Science, Springer Verlag, **152** (2000) pp. 41-156 .